

Cardiac Arrhythmia Detection and Classification Based on Subspace Approach and Neural Networks

Nadia Bouteraa, Salah Chenikher, Nouredine Doghmane and Messaoud Ramdani

Department of Electronics, Faculty of Engineering,

University Badji Mokhtar of Annaba, BP. 12, 23000, Annaba, Algeria

Abstract: This study presents a multi-stage system for reliable heart rhythm monitoring and diagnosis. It is comprised of three components including data pre-processing and feature extraction, abnormal arrhythmia detection and diagnosis. In the first stage, three different feature extraction methods are applied together to obtain a composite representation of the ECG waveform. In the second stage, the Multivariate Statistical Process Monitoring (MSPM) approach is used to capture the natural variations of the normal cardiac state and to detect any abnormal arrhythmia. Then a feed-forward neural network is used to classify the abnormal arrhythmia in 5 different classes. The results of experiments show the good performance of the proposed system.

Key words: Arrhythmia detection, heart beat classification, multi-features, multivariate statistical projection, neural network

INTRODUCTION

Electrocardiology has a fundamental role in cardiology since it consists of effective, non invasive, low-cost procedures for the detection, diagnosis and treatment of cardiac diseases. The cardiovascular pathological alterations observable by electrocardiology can be affected to three main groups: Cardiac rhythm disturbances (or arrhythmia), dysfunction of myocardial blood perfusion (or cardiac ischemia), chronic alternation of the mechanical structure of heart. Many cardiovascular diseases, caused by some kind of physical malfunction of one or several parts of the heart, have a reflection on the shape of the ECG signal. Thus, the ECG analysis has been particularly studied since it provides much information about the current state of the heart.

The ECG signal has a time periodicity which allows the definition of an individual beat composed by specific elementary waveforms. The study of the elementary waveforms and their dynamics constitutes the basis of the ECG signal analysis. The most striking waveform within the ECG is the QRS complex. Since it reflects the electrical activity within the heart during the ventricular contraction, the time of its occurrence as well as its shape provide rich information for the diagnosis. For instance, it serves as the basis for automated determination of the heart rate, as an entry point for classification schemes of

the cardiac cycle. In the same way, the time-distance between 2 consecutive QRS-complexes, known as RR-interval, is used to distinguish between certain types of cardiac rhythms. As a result, reliable ECG analysis depends heavily on the QRS detection step. In general, automatic ECG pattern recognition can be viewed as a sequential process involving two main steps: the feature extraction and the diagnosis task. Feature extraction can be regarded as a condensed representation of the initial pattern to some qualitative and quantitative features. Then, the classification is carried out, i.e., specific pattern is assigned to a specific class according to the characteristic features selected for it.

Within the last decade many methods to segment heartbeat automatically have been proposed (Hu and Tompkins, 1985; Thakor *et al.*, 1993). On the other hand, regarding the beat classification task, a large number of techniques have been previously reported, using a variety of features to represent the ECG and a number of classification methods. Features include interval features, frequency-based features, higher order cumulants, Karhunen-Loève expansion, orthogonal polynomials, autoregressive and wavelet based features. The classification techniques employed include linear discriminants, back-propagation neural networks, self-organizing maps with learning vector quantification, self-organizing networks and fuzzy logic.

In this study, a heart beat recognition system is proposed in which multiple features extracted from various descriptors were reduced in dimensionality by the well known linear subspace method, Principal Component Analysis (PCA) and a Feed-Forward Artificial Neural Network (FANN) we designed to classify heart beats into corresponding categories. The concerned arrhythmia categories are Normal beat (N), Premature Ventricular Contraction (PVC), Atrial Premature Contraction (APC), Left Bundle Branch Block (LBBB), Right Bundle Branch Block (RBBB) and Paced beat (P).

MATERIALS AND METHODS

The global scheme of the automatic heartbeat monitoring and classification presented in this research is composed of 3 main stages as shown in Fig. 1. The first step involves noise cancellation, R peak detection and beat segmentation in various waveforms for feature extraction. For a better characterization of the ECG waveform, multiple features are extracted simultaneously to form a composite vector. Then, the detection stage based on Multivariate Statistical Process Monitoring (MSPM) approach is used to detect abnormal arrhythmia. Finally, the neural network classifier will label the detected abnormal cardiac state as one of five classes of arrhythmia. Figure 2 displays samples of the arrhythmia categories under consideration.

ECG pre-processing and waveform description: The digitized ECG signals obtained from MIT-BIH arrhythmia database (Mark and Moody, 1988) were pre-processed with band pass filter of 1-100 Hz to remove baseline wander, power line interference and high frequency noises (Minami *et al.*, 1999). In order to detect R wave, peak detection process is employed (Hu and Tompkins, 1985; Thakor *et al.*, 1993). Centred on the detected R-wave peak, the ECG beats are extracted by applying a Hamming window with 128 samples of length. In general, automatic ECG beat recognition relies on several features extracted from ECG beat, mainly in the temporal domain, such as the width and height of QRS complex, RR interval, QRS area, etc. Since these temporal features are very sensitive to variations in morphology and temporal characteristics, other parameters can be extracted from the frequency domain, such as the measure of energy in a band of frequencies. The multi-resolution analysis has been also used extensively in recent years. In order to improve the system performance, a common way is to define some characteristic features in different domains that are more robust to variations of ECG morphology. Unfortunately, this is accompanied by an increase in the number of input

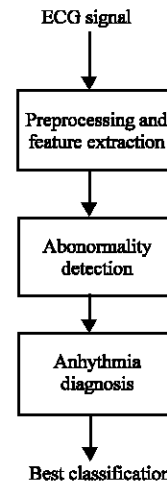


Fig. 1: Architecture of the proposed system

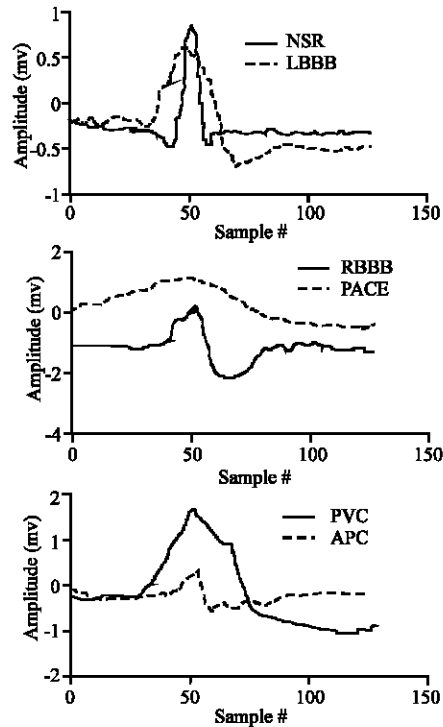


Fig. 2: ECG signals of 6 classes: Normal Sinus Rhythm beats (NSR); Left Bundle Branch Block Beats (LBBB), Right Bundle Branch Block Beats (RBBB); Pace beat (PACE); Premature Ventricular Contraction beats (PVC); Atrial Premature Contraction (APC)

features. This calls for an effective solution to select the most informative features for a possible reduction of the input dimension. To this end, the subspace approach can be used to handle the above issue. In the present study, three sets of features describing isolated ECG beats are

proposed as candidates to form a compact representation, which in its turn is reduced by subspace projection (Oja, 1983).

Linear prediction coefficients: A linear auto-regressive model can be used in time series analysis to predict the value of the next sample of a signal, the latter is taken as a linear combination of the previous samples. The next sample of the time series, S_k is predicted as the weighted sum of the p previous samples, $S_{k-1}, S_{k-2}, \dots, S_{k-p}$ and can thus be written:

$$s_k = \sum_{i=1}^p a_i s_{k-i} + e_k \quad (1)$$

Where a_1, a_2, \dots, a_p represent the model coefficients and p its order. The residual error, e_k , is a white noise of variance σ^2 and which represents the prediction error.

The Z-transform of the above equation reads:

$$S(z) \left(1 + \sum_{i=1}^p a_i z^{-i} \right) = E(z) \quad (2)$$

The signal s_k can thus be seen like the passage of white noise e_k of variance σ^2 through a filter of transfer function $H(z)$:

$$H(z) = \frac{1}{\left(1 + \sum_{i=1}^p a_i z^{-i} \right)} \quad (3)$$

The identification of the a_i coefficients can be performed by minimizing the mean square value of the residual errors over an analysis window. For the purpose of the study under consideration, the Burg algorithm has been used.

DWT based features: The Continuous Wavelet Transform (CWT) is defined as the integral of the signal $s(t)$ multiplied by scaled, shifted versions of a basic wavelet function $\psi(t)$:

$$c(a, t) = \int_{\mathbb{R}} s(t) \frac{1}{\sqrt{a}} \psi \left(\frac{t-b}{a} \right) dt, a \in \mathbb{R}^+ - \{0\}, b \in \mathbb{R} \quad (4)$$

Where, a is the so-called scaling parameters, b is the time localisation parameter. Associated with wavelet ψ , which is used to define the details in the decomposition, a scaling function ϕ is used to define the approximations. To avoid intractable computations of the CWT, scales and positions can be chosen based on a power of two, i.e. dyadic scales and positions. The Discrete Wavelet Transform (DWT) analysis is more

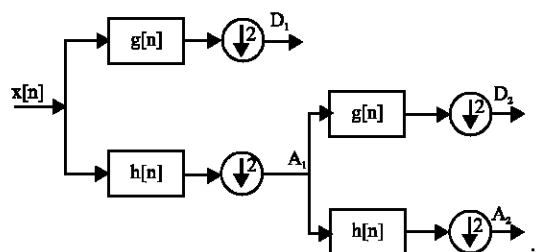


Fig. 3: Subband decomposition of discrete wavelet transform implementation; $g[n]$ is the high-pass filter, $h[n]$ is the low pass filter

efficient and accurate (Daubechies, 1998). In this scheme, the parameters a and b are given by:

$$(j, k) \in Z^2 : a = 2^j, b = k2^j, Z = \{0, \pm 1, \pm 2, \dots\}$$

This allows us to define

$$\psi_{j,k}(t) = 2^{-j/2} \psi(2^{-j}t - k), \phi_{j,k}(t) = 2^{-j/2} \phi(2^{-j}t - k) \quad (5)$$

A wavelet filter with impulse response g , plays the role of the wavelet ψ and a scaling filter with impulse response h , plays the role of scaling function ϕ . Figure 3 shows the principle of the dyadic wavelet decomposition. Thus, the DWT can be described mathematically as:

$$c(j, k) = \sum_{n \in Z} s(n) g_{j,k}(n) \quad (6)$$

$$a = 2^j, b = k2^j, j \in \mathbb{N}, k \in \mathbb{N}$$

The detail at level j is defined as:

$$D_j(t) = \sum_{k \in Z} c(j, k) \psi_{j,k}(t) \quad (7)$$

In practice, the decomposition can be determined iteratively, with successive approximations being computed, such that the analysed signal is decomposed into many lower-resolution components. In the present study, a five level DWT is defined and the normalized variances of the details coefficients are used as features.

Higher order statistics: Since the physiological signals, in general, are very complex and may be distributed according to Gaussian white and colour noises with unknown frequencies, the higher order statistics offer a promising way to minimize the effect of these noises. Assuming that the signal of interest has zero mean and discrete in time, three types of statistics have been taken

into account: the second-, third-and fourth order cumulants of a zero-mean stationary process are defined by Nikias and Petropulu (1993).

$$C_{2x}(k) = E\{x^*(n)x(n+k)\} \quad (8)$$

$$C_{3x}(k,l) = E\{x^*(n)x(n+k)x(n+l)\} \quad (9)$$

$$C_{4x}(k,l,m) = E\{x^*(n)x(n+k)x(n+l)x^*(n+m)\} \\ - C_{2x}(k)C_{2x}(l-m) - C_{2x}(l)C_{2x}(k-m) \\ - M_{2x}^*(m)M_{2x}(k-l) \quad (10)$$

Where E means the expectation operator and k, l, m⁻ the time lags $M_{2x}(k) = E\{x(n)x(n+k)\}$ and equals $C_{2x}(k)$ for a real-valued process. The first-order cumulant is the mean of the process and the second-order cumulant is the autocovariance sequence. The zero-lag cumulants have special names: $C_{2x}(0)$ is the variance and is usually denoted by σ^2 ; $C_{3x}(0,0)$ and $C_{4x}(0,0,0)$ are usually denoted by r_{3x} and r_{4x} . The normalized quantities, r_{3x}/σ^2 and r_{4x}/σ^4 are referred to as skewness and kurtosis, respectively. These normalized quantities are both time shift and scale invariant. In this research, we have extracted three points of the 3rd and 4th cumulants eventually distributed within the range of 15 lags.

Detection stage: Let us consider a process data matrix $X(N \times n)$ composed of N sample vectors with n variables measurements. Denote the correlation matrix of X as $\Sigma = X^T X / (N - 1)$ and performing Singular Value Decomposition (SVD) to the matrix Σ yields

$$\Sigma = UAU^T \quad (11)$$

Where, $U_{n \times n}$ is a unitary matrix and $\Lambda = \text{diag}(\lambda_1, \dots, \lambda_n)$ is a diagonal one containing the eigenvalues in decreasing order. The column vectors in the matrix $U = [u_1, \dots, u_n]$ form a new orthogonal base of space R^n and the first q ($q < n$) linear independence vectors.

$$\hat{P} = [u_1, u_2, \dots, u_q]$$

of U spans the principal component subspace \hat{S} . The other $n-q$ vectors

$$\tilde{P} = [u_{q+1}, u_{q+2}, \dots, u_n]$$

of U spans the residual subspace \tilde{S} . Selecting the correct number of principal components to retain in a

model is a nontrivial task and there are many subjective rules that can be used to help with this task. The number of principal components to retain can be selected as its Cumulative Percent Variance (CPV) is larger than a prescribed threshold (Jackson and Mudholkar, 1979). The data vector $x \in R^n$ can be decomposed as

$$x = \hat{x} + \tilde{x} = \hat{C}x + \tilde{C}x \quad (12)$$

Where, $\hat{x} \in \hat{S}$ and $\tilde{x} \in \tilde{S}$ are projection of x on the subspaces \hat{S} and \tilde{S} , respectively. The matrix

$$\hat{C} = \hat{P}\hat{P}^T \text{ and } \tilde{C} = \tilde{P}\tilde{P}^T$$

are the corresponding projection operators. The score vector in the space model space

$$z = \hat{P}^T x \in R^q$$

is a reduced, q-dimensional representation of the observed vector x. More specifically, the jth principal component is

$$z_j = p_{1j}x_1 + p_{2j}x_2 + \dots + p_{nj}x_n \quad (13)$$

Where p_{ij} is the weight value that reflects the contribution of x_i to a PC z_j . As tried by this study, PCs that were extracted from data reduction through PCA can be used as inputs to the next step analysis. The PCA statistical monitoring model is build on two hypothesis tests in subspaces \hat{S} and \tilde{S} . The statistic used in \hat{S} is the Hotelling T^2 which is defined as

$$T^2 = \|\Lambda_q^{-1/2} \hat{P}x\| \leq T_{lim}^2 \quad (14)$$

With $\Lambda_q = \text{diag}(\lambda_1, \dots, \lambda_q)$. The statistic used in \tilde{S} is the Q-statistic or the Sum of Prediction Error (SPE), which is defined as below

$$SPE = \|\tilde{C}x\| \leq \delta_\alpha^2 \quad (15)$$

Where δ_α^2 is the control limit for SPE index. The 100 (1- α)% control limit for T^2 is calculated by means of an F-distribution as follows:

$$T_{lim}^2 = \frac{q(N-1)}{N-q} F(q, N-1, \alpha) \quad (16)$$

Where, $F(q, N-1, \alpha)$ is an F-distribution with degrees of freedom q and N-1 and with level of significance α . A confidence limit expression for SPE can be computed from its approximate distribution (Jackson and Mudholkar, 1979):

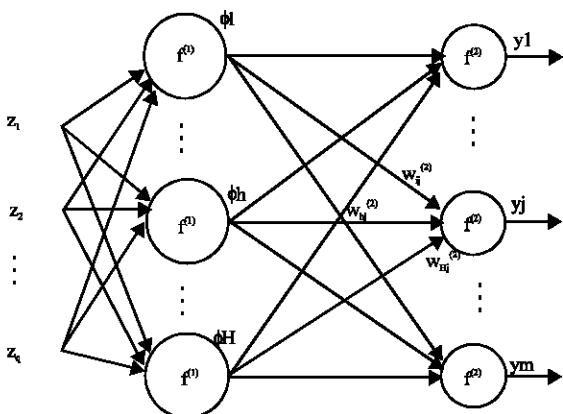


Fig. 4: Architecture of the Feedforward Artificial Neural Network (FANN) classifier

$$\delta_{\alpha}^2 = g \lambda_{h,\alpha}^2 \tag{17a}$$

$$g = \theta_2 / \theta_1 \tag{17b}$$

$$h = \theta_1^2 / \theta_2 \tag{17c}$$

Where, $\theta_i = \sum_{j=q+1}^n \lambda_j^i$ for $i=1,2$

Classification stage: Once an abnormal arrhythmia is detected, the projection of the feature vector describing the ECG waveform in the principal component subspace is fed to the classification stage. The employed classifier was a feed-forward artificial neural network (Fig. 4) with one hidden layer with appropriate number of hidden neurons (Hartman *et al.*, 1990; Poggio and Girosi, 1990). The input of the network is formed by the vector

$$\bar{z} = (z_1, \dots, z_q)^T$$

Where, q is the number of input variables. In this case, \bar{z} is the score vector of a composite vector \bar{x} including three representations, i.e. autoregressive coefficients, the parameters derived from the discrete wavelet transform and higher order statistics. The j th output of the network, y_j , is defined by the following equations:

$$y_j = f^{(2)}(a_j); a_j = \sum_{h=1}^H w_{jh}^{(2)} \phi_h + w_{j0}^{(2)}; j = 1, \dots, C \tag{18}$$

$$\phi_h = f^{(1)}\left(\sum_{i=1}^q w_{hi}^{(1)} z_i + w_{h0}^{(1)}\right); h = 1, \dots, H$$

Where C is the number of hidden neurons, the super index indicates the number of layer, w are the weights of the neural network and $f^{(1)}$ and $f^{(2)}$ are the activation functions of the neurons of the hidden and output layers, respectively. In this research, the hyperbolic tangent function was used for $f^{(1)}$ and the soft-max activation function was used for $f^{(2)}$, because this makes possible to interpret the outputs as probabilities and is defined as:

$$f^{(2)}(a_j) = \frac{e^{a_j}}{\sum_{k=1}^C e^{a_k}} \tag{19}$$

With the aim of obtaining the optimal set of values for the network weights that minimizes the error function for a given training data while having a good generalisation ability for unseen data, the following cost function is employed:

$$E(\bar{w}) = E_D(\bar{w}) + \alpha E_w(\bar{w}) \tag{20}$$

It is defined as a regularized maximum likelihood cost function, in which the $E_D(\bar{w})$ term measures the error obtained when the output of the network is compared with the target. In this study, the cross-entropy error function has been used as it is the more suitable for classification tasks. Therefore, $E_D(\bar{w})$ is defined as:

$$E_D(\bar{w}) = -\sum_{k=1}^N \sum_{j=1}^C t_j^{(k)} \ln(y_j(w, z^{(k)})) \tag{21}$$

Where N is the number of training data, C the number of classes,

$$\{(z^{(k)}, t^{(k)})\}$$

is the set of training pairs; $z^{(k)}$ is the k th input vector and $t^{(k)}$ its expected output given by:

$$t_j^{(k)} = \begin{cases} 1 & \text{if } z^{(k)} \in C_j \\ 0 & \text{otherwise} \end{cases} \tag{22}$$

The second term in (11), $E_w(\bar{w})$ is a regularization term called weight decay, defined as:

$$E_w(\bar{w}) = \frac{1}{2} \sum_{i=1}^{N_w} w_i^2 \tag{23}$$

Where, N_w is the number of weights of the neural network and w_i the i th component of \bar{w} . The use of this term avoids the over fitting problem and thus it improves the generalisation of the network.

THE RESULTS OF NUMERICAL EXPERIMENTS

The ECG records with normal beats and different types of arrhythmia are selected from the MIT/BIH arrhythmia database (Mark and Moody, 1988). The MIT-BIH ECG records are 2 channels, 30 min duration, sampled at 360 samples/s per channel with 11-bit resolution over a 10 mV range. Two or more cardiologists independently annotated each record; disagreements were resolved to obtain the computer-readable annotations for each beat. Each type heartbeat was extracted from the record which contained most beats of this type. In our experiment, six different types of ECG classes including Normal (N), Left Bundle Branch Block (LBBB), Right Bundle Branch Block (RBBB), Pace beat (PACE), Premature Ventricular Contraction (PVC) and Atrial Premature Contraction (APC) beats are extracted, respectively from five ECG records (files numbered 100, 109, 118, 107, 208 and 232).

The selected ECG beats being classified have been divided in two groups: One used for the learning purposes and the other for testing the performance of the classifier. Table 1 shows the selected ECG beats. Due to the scarcity of data corresponding to some beat types the number of data belonging to each beat type is variable. Table 2 shows the result of classification for all classes of heart beats for the combined used of PCA-FANN. In PCA-FANN, the PCA is used for dimensionality reduction and the feed-forward artificial neural network as a classifier. Figure 5 shows the eigenvalues and the,

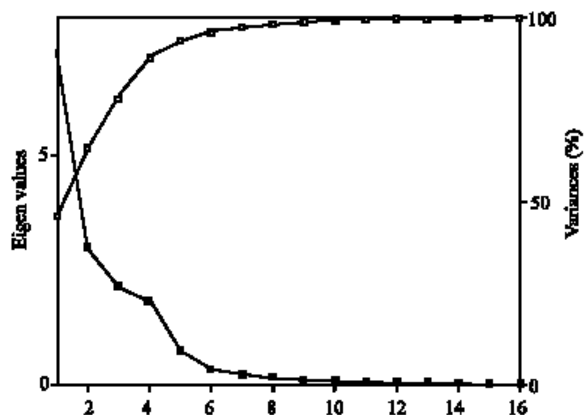


Fig. 5: Eigenvalues and respective cumulative variances %

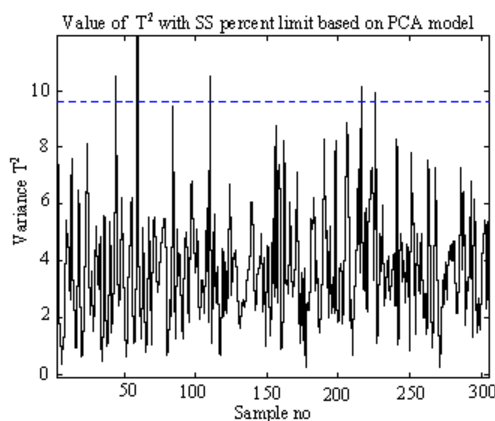


Fig. 6: The T^2 statistic (solid line) and its control limit (dashed line)

Table 1: The selected beats

Beat type	Training beats	Testing beats
Normal (N)	677	560
LBBB	739	751
RBBB	654	510
PACE	656	420
PVC	300	290
APC	435	345
Total	2284	2876

Table 2: Overall performance of the proposed system PCA-FANN in testing mode

Beat type	Classified	Accuracy (%)
Normal	547	97.68
LBBB	738	98.27
RBBB	504	98.82
PACE	409	97.38
PVC	290	100
APC	340	98.95
Total	2828	98.51

Table 3: Comparative results of ECG beat classifiers

	Number of beat types	Efficiency
MLP-Fourier (Minami <i>et al.</i> , 1999)	3	98
SOM-SVD (Hu <i>et al.</i> , 1997)	4	92.2
Fhyb-HOSA (Osowski and Linh, 2001)	7	96.06
PCA-FANN	6	98.51

respective cumulative variances %. The T^2 statistic and its control limit for the training normal beats dataset are given in Fig. 6. For the same dataset the SPE statistic and its control limit are given in Fig. 7. It is worth noticing that for some samples (beats) the 2 statistics are higher than their control limits and this generates false detection alarms. This means that the linear model has failed to certain extent to capture the natural variations of the normal beats. Obviously, a false alarm can be confirmed or not by the classification module.

To evaluate the performance of the detection module, a subset of normal beats followed by an abnormal rhythms is used to compute the SPE statistic as shown in Fig. 8.

The average misclassification rate for both learning and test sets is very small and the recognition rate in the test mode is approximately 98.51%. In order to compare the obtained results with other techniques. Table 3 summarizes the comparative results between the following

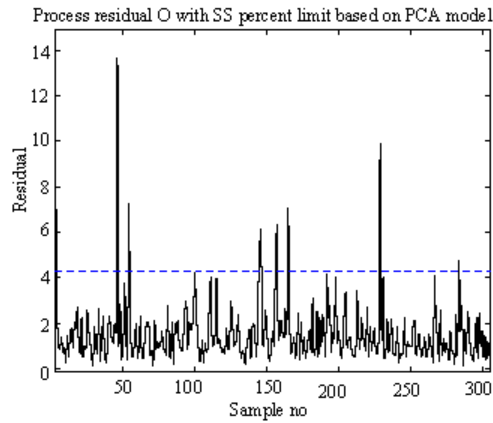


Fig. 7: The SPE statistic (solid line) and its control limit (dashed line)

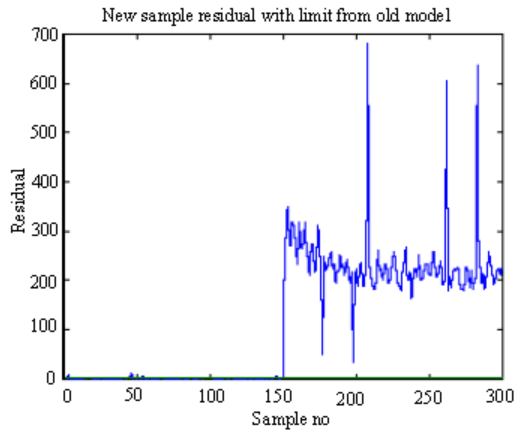


Fig. 8: The SPE statistic and its control limit for 150 normal beats followed by 150 abnormal rhythms of the LBBB class

classifiers: Multi-Layer Perceptron with Fourier transform (MLP-Fourier) (Hu *et al.*, 1997), Self-Organizing Maps and Singular Value Decomposition (SOM-SVD) (Osowski and Linh, 2001), Fuzzy hybrid neural network (Fhyb-HOSA) (Minami *et al.*, 1999), PCA-FANN. However, it is interesting to mention that patients and rhythms selected in all compared experiments were different. Hence fair comparison of the classifiers and their results is very difficult. Moreover, since different numbers of beat types have been used in the above methods, the second column of Table 3 gives the number of these beat types or classes and column 3 shows the overall recognition rate.

CONCLUSION

This study describes a new system for the detection and the classification of cardiac arrhythmia using the subspace approach and artificial neural networks in order to improve the quality of the diagnosis. The results from a relatively large dataset of actual ECG signals from 6 different classes showed that the proposed system gives good performances. Future research should address the use of a nonlinear generalisation of PCA to overcome the limitations of global linear PCA as well as more sophisticated classification schemes to improve the results.

REFERENCES

- Daubechies, I., 1998. Orthonormal bases of compactly wavelets. *Commun. Pure Applied Math.*, 41: 909-996.
- Hartman, E.J., J.D. Keeler and J.M. Kowalsky, 1990. Layered neural networks with Gaussian hidden units as universal approximators. *Neural Comput.*, 2: 210-215.
- Hu, Y.H. and W. Tompkins, 1985. A real time QRS detection algorithm. *IEEE. Trans. Biomed. Eng.*, 32: 230-236.
- Hu, Y.H., S. Palreddy and W. Tompkins, 1997. A patient adaptable ECG beat classifier using a mixture of experts approach. *IEEE. Trans. Biomed. Eng.*, 44: 891-900.
- Jackson, J.E. and G.S. Mudholkar, 1979. Control procedures for residuals associated with principal component analysis. *Technometrics*, 21: 3.
- Mark, R. and G. Moody, 1988. *MIT-BIH Arrhythmia Database Directory*, Cambridge, MA: MIT.
- Minami, K., H. Nakajima and T. Toyoshima, 1999. Real-time discrimination of Ventricular tachyarrhythmia with Fourier transform neural network. *IEEE. Trans. Biomed. Eng.*, 46: 179-185.
- Nikias, C. and A. Petropulu, 1993. *Higher order spectral analysis*, Prentice Hall, N.J.
- Oja, E., 1983. *Subspace Methods of Pattern Recognition*. Research Studies Press, England.
- Osowski, S. and T.H. Linh, 2001. ECG beat recognition using fuzzy hybrid neural network. *IEEE. Trans. Biomed. Eng.*, 48: 1265-1271.
- Poggio, T. and F. Girosi, 1990. Networks for approximation and learning. *Proc. IEEE.*, 78: 1481-1497.
- Thakor, N.V., J.G. Webster, W.J. Tompkins, 1993. Optimal QRS detector. *Med. Biol. Eng. Comput.*, 21: 343-350.